Electronic Supplementary Material (ESI) for Chemical Science.
This journal is © The Royal Society of Chemistry 2019

Electronic Supplementary Information (ESI)

Clustering-triggered emission strategy towards tunable multicolor persistent phosphorescence

Qing Zhou, Tianjia Yang, Zihao Zhong, Fahmeeda Kausar, Ziyi Wang, Yongming Zhang and Wang Zhang Yuan**

School of Chemistry and Chemical Engineering, Shanghai Key Lab of Electrical Insulation and Thermal Aging, Shanghai Electrochemical Energy Devices Research Center, Shanghai Jiao Tong University, Shanghai 200240, China

E-mail: ymzhang@sjtu.edu.cn (Y.Z.); wzhyuan@sjtu.edu.cn (W.Z.Y.)

Experimental Section

Materials. Glycerol (Gly) (98%) and pentaerythritol (PER) (98%) were purchased from Acamas-Beta. D-galactose (D-Gal) (99%), D-fructose (D-Fru) (99%) and D-Xylose (D-Xyl) (98%) were provided by Shanghai Maclean Biochemical Technology Co., Ltd. All above compounds were further purified before use. Acetone, tetrahydrofuran (THF) and anhydrous ethyl ether were bought from Sinopharm Group Co., Ltd, which were distilled before use. Purified water was purchased from Hangzhou Wahaha Group Co., Ltd and used as received.

Instrumentation. ^{1}H and ^{13}C NMR spectra were measured on a Bruker ARX 500 NMR spectrometer using D_2O as solvent. Absorption spectra of solutions were taken on a Lambda 35 UV-Vis spectrometer (Perkin Elmer, USA). Prompt photoluminescence (PL) spectra at room temperature were recorded by a PerkinElmer LS55 fluorescence spectrophotometer. Delayed PL spectra of crystals at room temperature (D-Xyl, PER, D-Fru, D-Gal) and 77 K (D-Xyl, PER), phosphorescence lifetimes

and quantum efficiencies (Φ) were measured on an Edinburgh FLS1000 fluorescence spectrometer. PL and delayed PL spectra of aqueous D-Xyl solution (1 M) at 77 K were recorded on a HORIBA high sensitivity integrated fluorescence spectrometer FluoroMax-4. The Φ values were measured with optimal excitation wavelengths ($\lambda_{ex,o}$) for concentrated aqueous solutions of D-Xyl (1 M, 1×10^{-4} M), PER (0.1 M, 1×10^{-4} M), D-Fru (1 M, 1×10^{-4} M) and D-Gal (1 M, 1×10^{-4} M) and their crystals via an integrating sphere. Fluorescence lifetimes at nanosecond scale were acquired with a QM/TM/IM steady-transient time-resolved spectroscopy (PTI, USA). The data were well fitted by the single exponential decay nfunction *via* the Origin Pro software. Crystallography data for D-Xyl, PER, D-Gal and D-Fru were collected on a Bruker D8 Venture-CMOS diffractometer with CuK X-ray source radiation (λ = 1.54184 Å) at room temperature in the ω scan mode. Luminescent photographs were taken with a SLR camera (Canon EOS 70D, Japan), and the videos were recorded using acamera (Sony A7S2, Japan) and the afterglow images were captured from the videos.

Sample Purification. (1) Gly was purified by distillation under reduced pressure at 175 °C. (2) D-Xyl, PER and D-Gal: Their powders were dissolved in purified water at room temperature, and then recrystallized with THF (poor solvent) to obtain the precipitates. (3) D-Fru: Firstly, its powders were dissolved in a mixture of purified water and ethanol, and then recrystallized by adding ethyl ether. The precipitates were obtained at 4 °C in a refrigerator. Then all four obtained precipitates were filtered through a sand core funnel and then freeze-dried in vacuum at room temperature 72 h.

Cultivation of Single Crystals. (1) D-Xyl, PER and D-Gal single crystals were obtained by a solvent evaporation method from their aqueous solution. (2) D-Fru single crystal was obtained by a solvent evaporation method from its ethanol solution. The aqueous solutions were prepared from the purified powders.

Calculation of HOMO and LUMO Electron Densities. The Gaussian 09 program was utilized to perform the TD-DFT calculations of the monomer, dimer, trimer and tetramer of D-Xyl at the TD-B3LYP/6-31G* level. The molecular structures adopted from the single crystal data without further

geometry optimization were used for the calculation. The HOMO and LUMO energy densities were obtained via GaussView 5.0.8 (isovalue-0.02, cube grid-coarse). Similar method was utilized for the calculation of PER.

NMR Characterization

(i) PER. ^{1}H NMR (500 MHz, D_2O) δ 3.61 (s, 8H). ^{13}C NMR (126 MHz, D_2O) δ 45.33, 60.94.

(ii) D-Xyl. ^{1}H NMR (500 MHz, D_2O) δ 3.22 (dd, *J* = 9.3, 7.9 Hz, 1H), 3.32 (t, *J* = 11.1 Hz, 1H), 3.43 (t, *J* = 9.3 Hz, 1H), 3.52 (dd, *J* = 9.3, 3.7 Hz, 1H), 3.60 (d, *J* = 6.6 Hz, 1H), 3.61–3.71 (m, 4H), 3.92 (dd, *J* = 11.5, 5.5 Hz, 1H), 4.57 (d, *J* = 7.9 Hz, 1H), 5.19 (d, *J* = 3.6 Hz, 1H). ^{13}C NMR (126 MHz, D_2O) δ 60.92, 65.17, 69.21, 69.39, 71.45, 72.81, 74.02, 75.80, 92.21, 96.60.

(iii) D-Fru. ^{1}H NMR (500 MHz, D_2O) δ 3.45 (d, *J* = 6.4 Hz, 1H), 3.47 (d, *J* = 6.0 Hz, 1H), 3.50 (d, *J* = 10.1 Hz, 1H), 3.55–3.60 (m, 1H), 3.60 (d, *J* = 1.8 Hz, 1H), 3.63 (d, *J* = 2.7 Hz, 1H), 3.69 (d, *J* = 3.6 Hz, 1H), 3.72 (d, *J* = 5.4 Hz, 1H), 3.79 (s, 1H), 3.79–3.82 (m, 1H), 3.90 (d, *J* = 1.6 Hz, 1H), 3.91 (dd, *J* = 6.9, 1.5 Hz, 1H), 3.95 (d, *J* = 1.4 Hz, 1H), 4.01 (dd, *J* = 3.9, 2.8 Hz, 1H). ^{13}C NMR (126 MHz, D_2O) δ 61.08, 62.36, 62.65, 62.90, 63.34, 63.87, 67.54, 69.18, 69.66, 74.43, 75.37, 76.02, 80.65, 81.28, 81.94, 98.04, 101.47, 104.41.

(iv) D-Gal. ^{1}H NMR (500 MHz, D_2O) δ 3.38 (ddd, *J* = 9.8, 6.3, 2.3 Hz, 1H), 3.57 (t, *J* = 9.7 Hz, 3H), 3.66 (dd, *J* = 9.7, 3.4 Hz, 1H), 3.74–3.88 (m, 5H), 3.89–3.93 (m, 1H), 3.93–3.96 (m, 1H), 4.89 (d, *J* = 1.1 Hz, 1H), 5.18 (d, *J* = 1.7 Hz, 1H). ^{13}C NMR (126 MHz, D_2O) δ 60.95, 61.16, 68.32, 68.72, 69.14, 69.28, 70.45, 71.85, 72.77, 75.12, 92.25, 96.42.

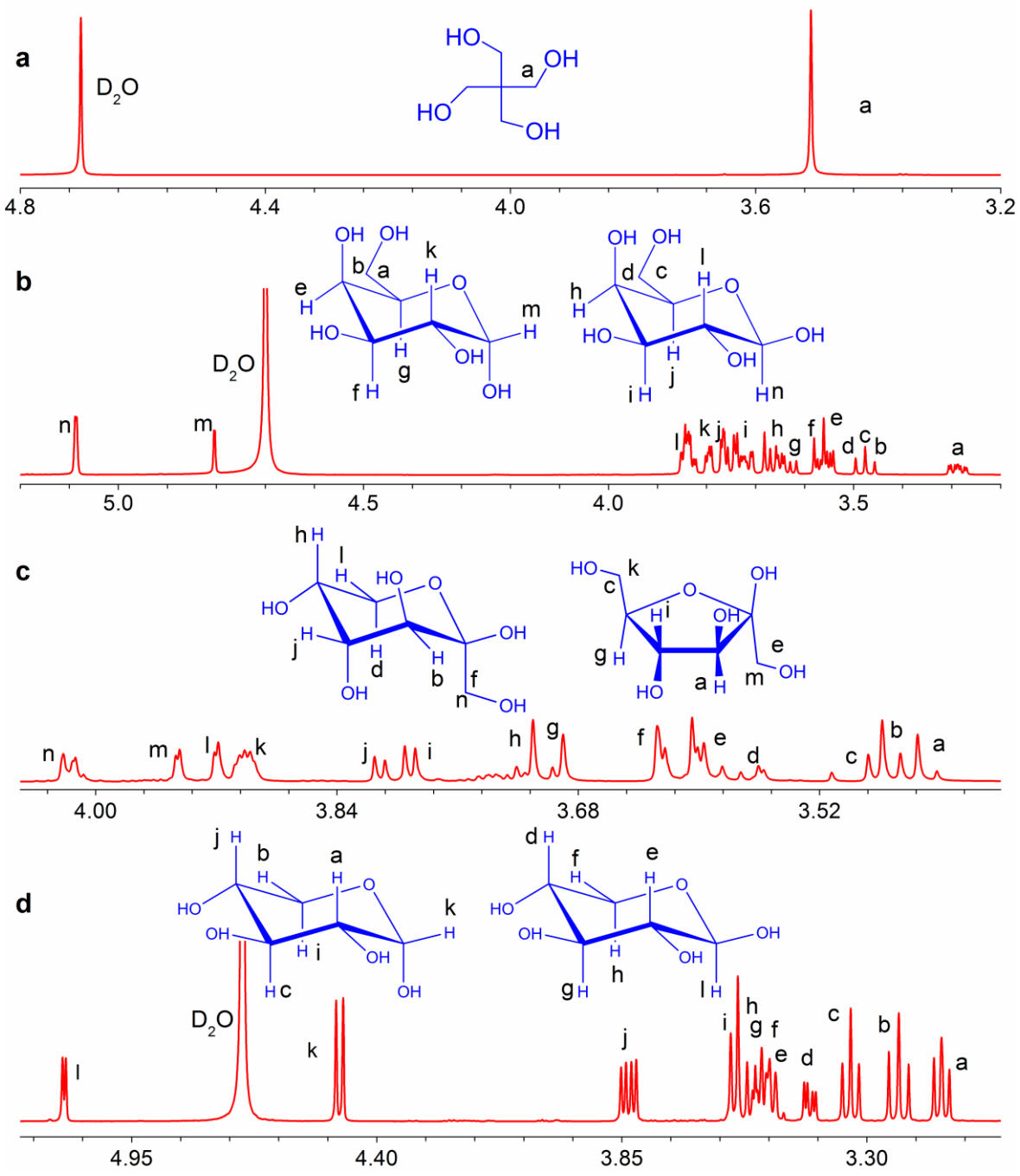

Fig. S1 ^{1}H NMR spectra of (a) PER, (b) D-Gal, (c) D-Fru and (d) D-Xyl.

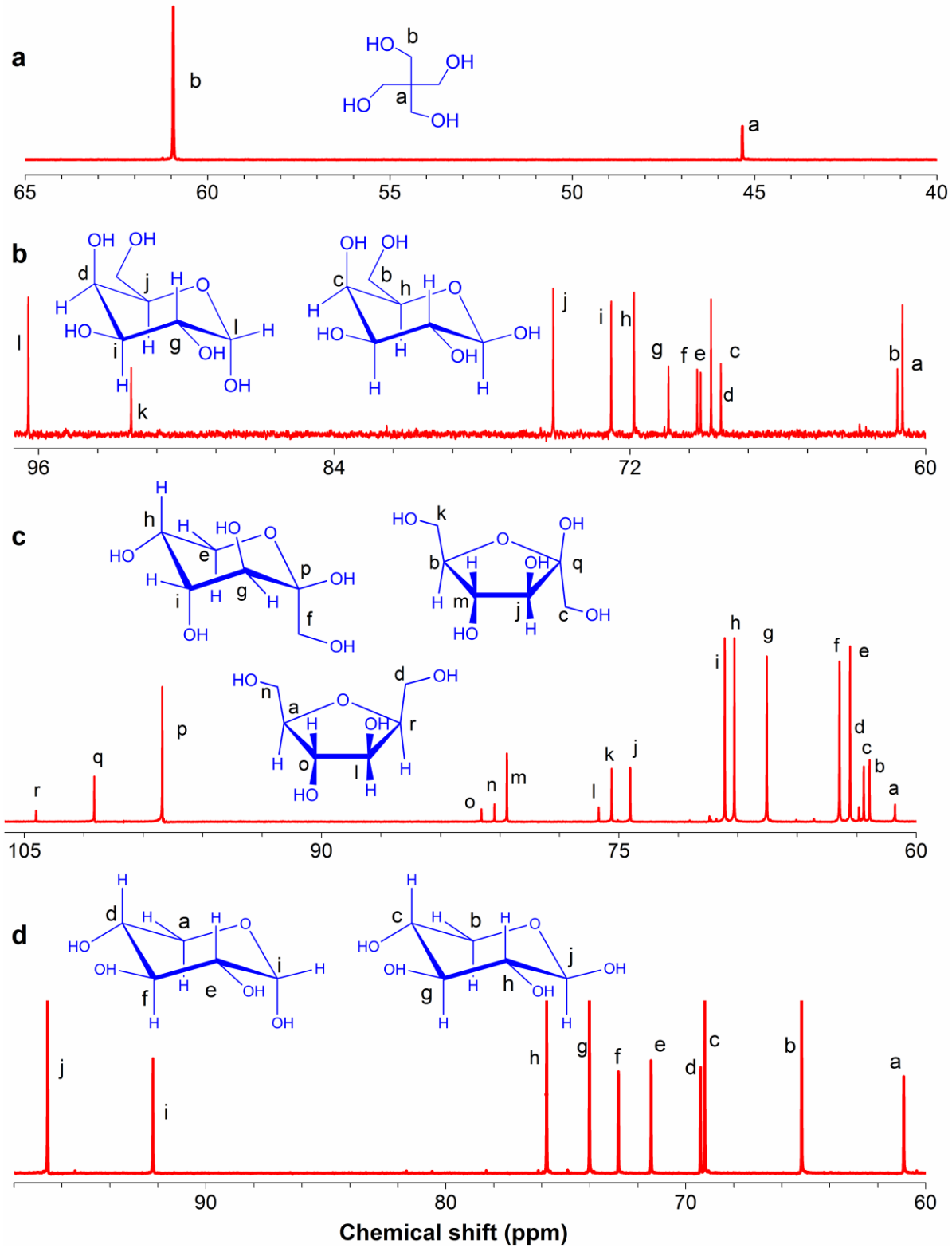

Fig. S2 ^{13}C NMR spectra of (a) PER, (b) D-Gal, (c) D-Fru and (d) D-Xyl.

Table S1. Single crystal data of D-Xyl, PER, D-Fru and D-Gal.

Compound reference	D-Xyl	PER	D-Fru	D-Gal
Chemical formula	$C_5H_{10}O_5$	$C_5H_{12}O_4$	$C_6H_{12}O_6$	$C_6H_{12}O_6$
Formula Mass	150.13	136.15	180.16	180.16
Crystal system	Orthorhombic	Tetragonal	Orthorhombic	Orthorhombic
a/Å	5.61070(10)	6.0826(12)	8.091(2)	7.7012(2)
b/Å	9.1858(2)	6.0826(12)	9.212(2)	7.7746(2)
c/Å	12.5998(3)	8.792(2)	10.056(2)	12.6751(4)
α/°	90.00	90.00	90.00	90.00
β/°	90.00	90.00	90.00	90.00
γ/°	90.00	90.00	90.00	90.00
Unit cell volume/Å^3	649.38(2)	325.31(15)	749.5(3)	758.91(4)
Temature/K	293(2)	298(2)	293(2)	297(2)
Space group	P2(1)2(1)2(1)	I-4	P2(1)2(1)2(1)	P2(1)2(1)2(1)
No. of formula units unit cell, *Z*	4	2	4	4
No. of reflections measured	4725	1675	5684	10058
No. of independent reflections	1065	304	1366	1378
R_{int}	0.0270	0.0423	0.0866	0.0862
Final R_1 values ($I > 2\sigma(I)$)	0.0302	0.0297	0.0656	0.0283
Final $wR(F^2)$ values ($I > 2\sigma(I)$)	0.1027	0.0801	0.1799	0.0804
Final R_1 values (all data)	0.0308	0.0354	0.0714	0.0287
Final $wR(F^2)$ values (all data)	0.1031	0.0836	0.1864	0.0810

$R_1 = \sum \| F_0 | - | F_c \| / \sum | F_0 |; wR_2 = \left\{ \sum \left[w \left(F_0^2 - F_c^2 \right)^2 \right] / \sum \left[\left(F_0^2 \right) \right]^2 \right\}^{1/2}$

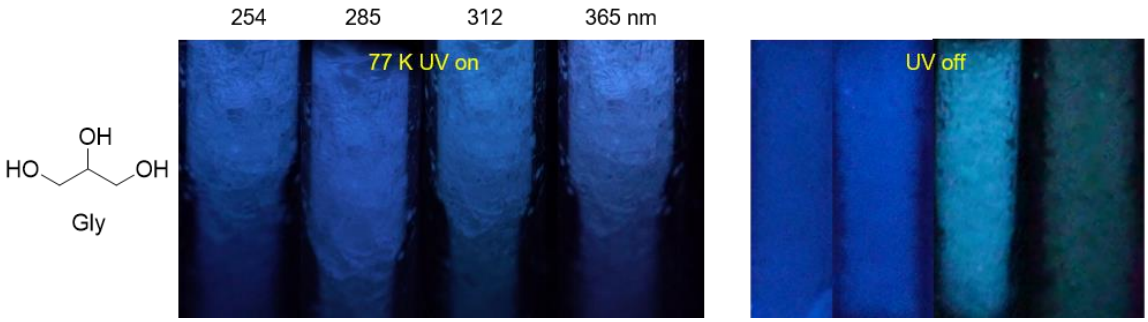

Fig. S3 Photographs of pure Gly taken at 77 K under varying UV lights (left) or after ceasing the UV irradiation (right).

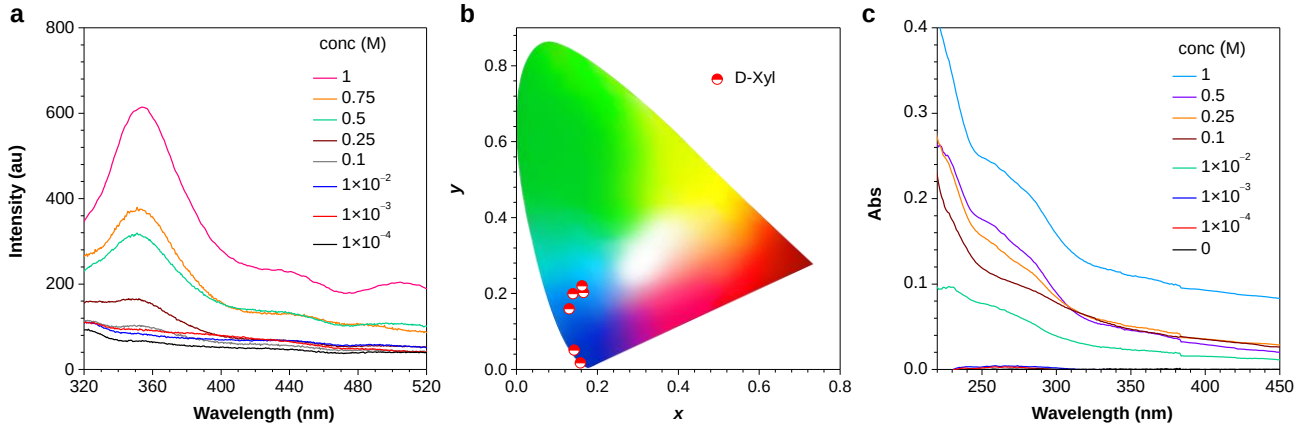

Fig. S4 (a) Emission spectra of aqueous D-Xyl solutions at varying concentrations (λ_{ex} = 284 nm). (b) Trajectory of color modulation of aqueous D-Xyl solutions, recorded by the change in the excitation from 252 to 365 nm, in the CIE coordinate diagram. (c) Absorption of aqueous D-Xyl solutions at varying concentrations.

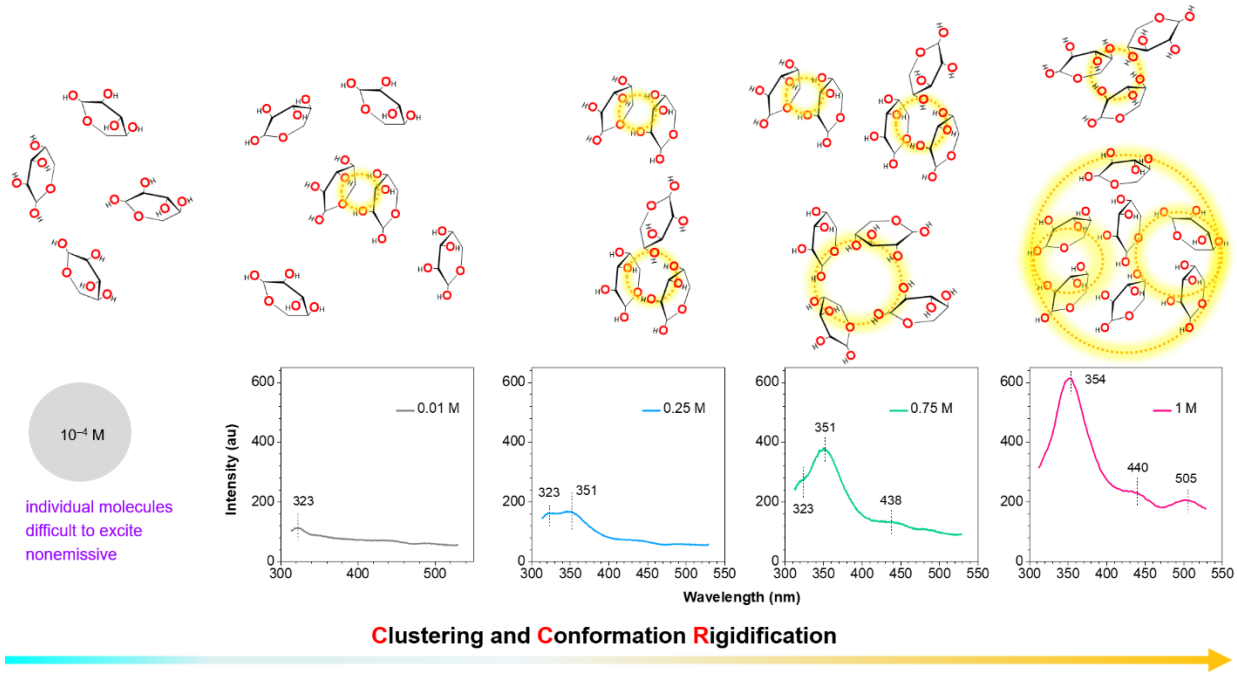

Fig. S5 Schematic illustration of the intrinsic relation between the concentration-enhanced emission and CTE mechanism utilizing D-Xyl (λ_{ex} = 284 nm).

The formation of oxygen clusters with sufficiently rigidified conformation is responsible for the emission in the concentrated solutions. As illustrated in Fig. S5, in very dilute solutions, individual D-Xyl molecules are difficult to excite owing to their short intramolecular through-space conjugation.

Meanwhile, even being excited, active intramolecular motions will effectively consume the exciton energy, thus making the dilute solutions barely emissive. While in concentrated solutions, D-Xyl molecules are clustered in close proximity one another, thus resulting in extended electronic conjugation and simultaneously rigidified conformations. These clusters facilitate the excitation and subsequent radiative deactivation upon irradiation, thus generating noticeable emission. The higher the concentration is, the more the clusters are formed, thereby offering much brighter emission.

***Note*:** Herein, water molecules should also take part into the formation of clusters, for simplicity, they were omitted.

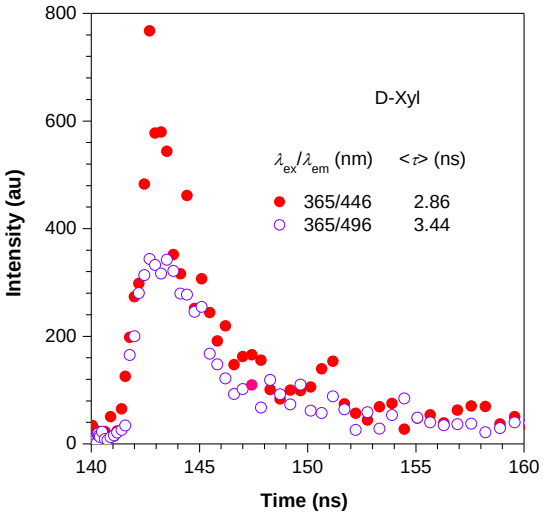

Fig. S6 Lifetime profiles of 1 M aqueous solution of D-Xyl monitored at different wavelengths.

Table S2. Summary of the ns scale lifetimes of the aqueous solution and crystals at ambient conditions.

Samples	τ [ns]	λ_{ex} [nm]	λ_{em} [nm]
D-Xyl (1 M)	2.86	365	446
	3.44	365	496
D-Xyl (crst)	2.75	340	428
	3.15	340	484
PER (crst)	2.39	330	420
	2.59	330	485
D-Fru (crst)	2.70	340	420
	3.07	340	485
D-Gal (crst)	2.70	340	395
	2.92	340	485

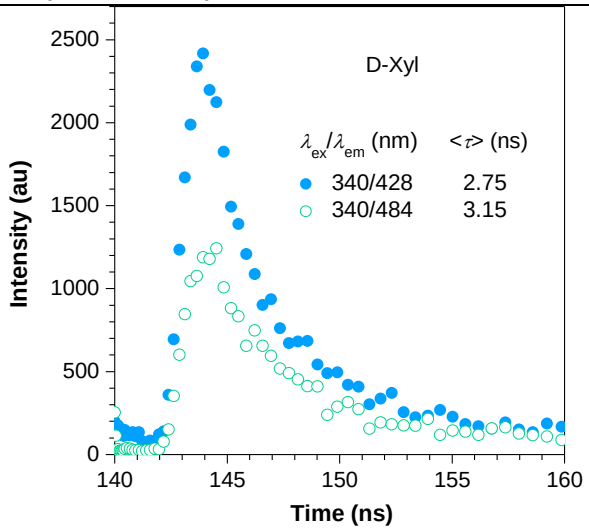

Fig. S7 Lifetime profiles of D-Xyl crystals monitored at different wavelengths.

Table S3. Summary of the *p*-RTP lifetimes of D-Xyl crystals.[a]

τ_1 [ms]	A_1 [%]	τ_2 [ms]	A_2 [%]	τ_3 [ms]	A_3 [%]	τ [ms]	$\lambda_{ex,RTP}$ [nm]	$\lambda_{em,RTP}$ [nm]
58.6	4.33	159.5	15.2	664.1	80.5	639.6	255	435
67.1	28.8	338.6	41.9	739.4	29.3	554.5	255	470
24.6	41.2	66.9	43.5	286.3	15.4	177.8	285	510
29.3	51.6	92.6	26.9	273.8	21.5	190.5	315	525

[a] All measurements were conducted at ambient conditions. $\lambda_{ex,RTP}$ = excitation wavelength used for the lifetime measurement; $\lambda_{em,RTP}$ = monitored emission wavelength. $\tau = (A_1\tau_1^2 + A_2\tau_2^2 + A_3\tau_2^3)/(A_1\tau_1 + A_2\tau_2 + A_3\tau_3)$. Longest τ_3 was adopted for *p*-RTP lifetimes in the manuscript.

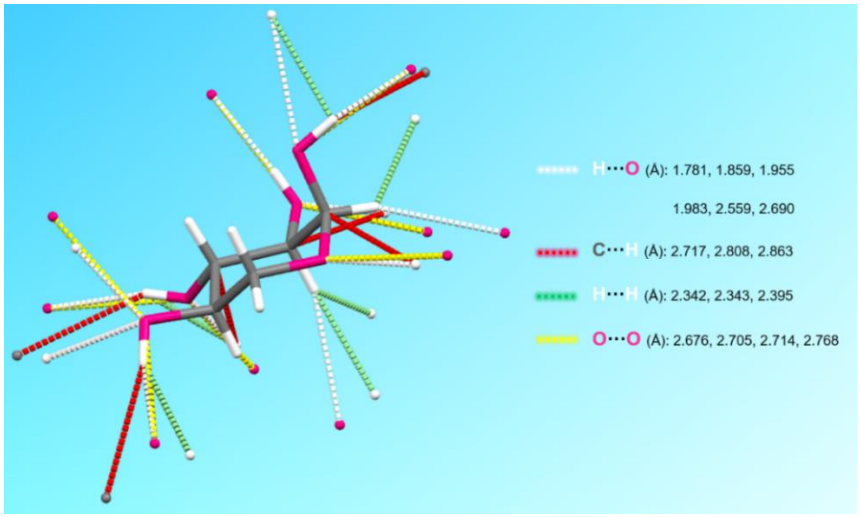

Fig. S8 Single crystal structure of D-Xyl with denoted intermolecular interactions.

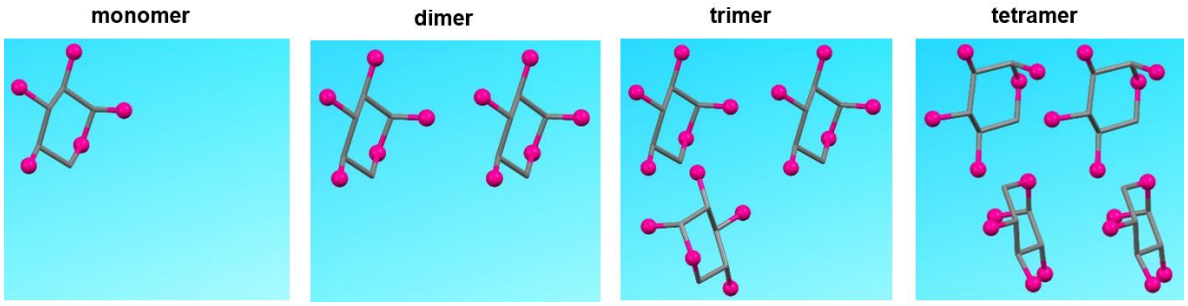

Fig. S9 Monomer, dimer, trimer and tetramer of D-Xyl adopted for calculation.

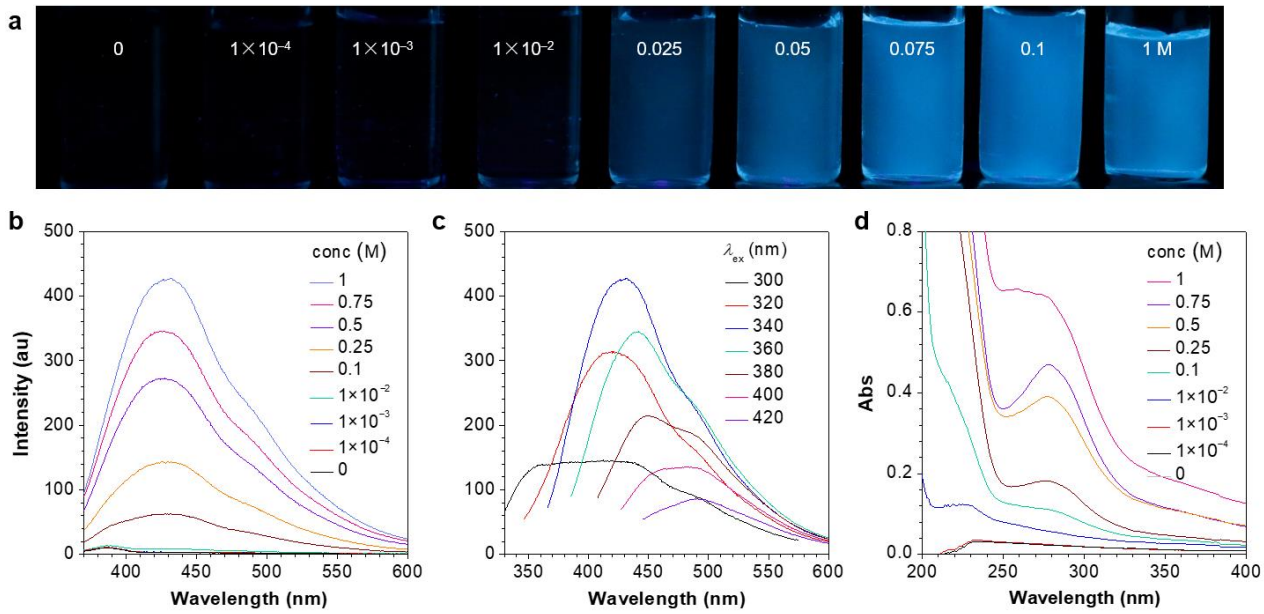

Fig. S10 (a) Photographs taken under 365 nm UV light and (b) Emission spectra of aqueous D-Gal solutions at varying concentrations (λ_{ex} = 340 nm). (c) Emission spectra of 1 M aqueous D-Gal solution with different λ_{ex}s. (d) Absorption of aqueous D-Gal solutions at varying concentrations.

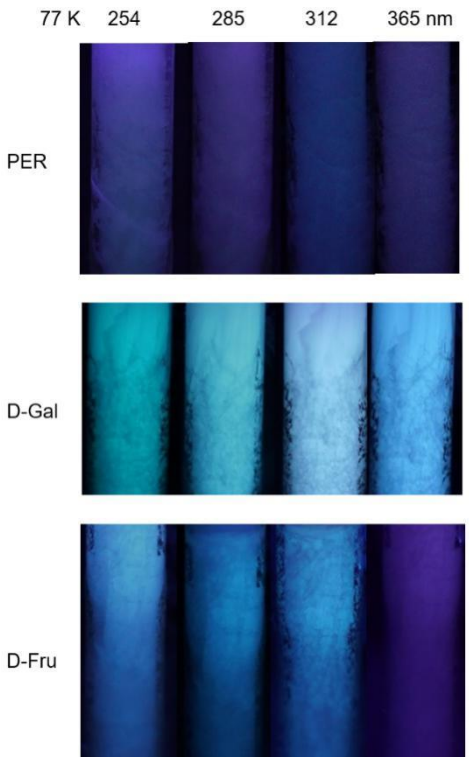

Fig. S11 Photographs of PER, D-Fru and D-Gal concentrated solutions under UV light at 77 K.

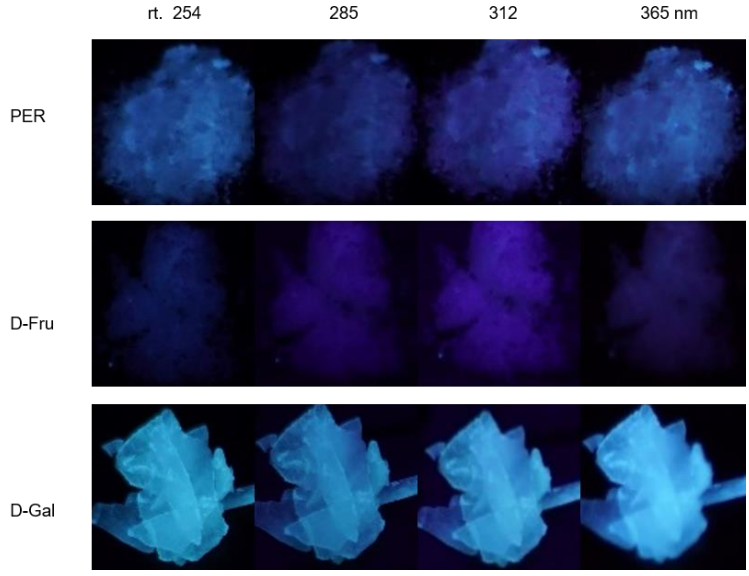

Fig. S12 Photographs of PER, D-Fru and D-Gal crystals taken under 254, 285, 312 and 365 nm UV lights at room temperature.

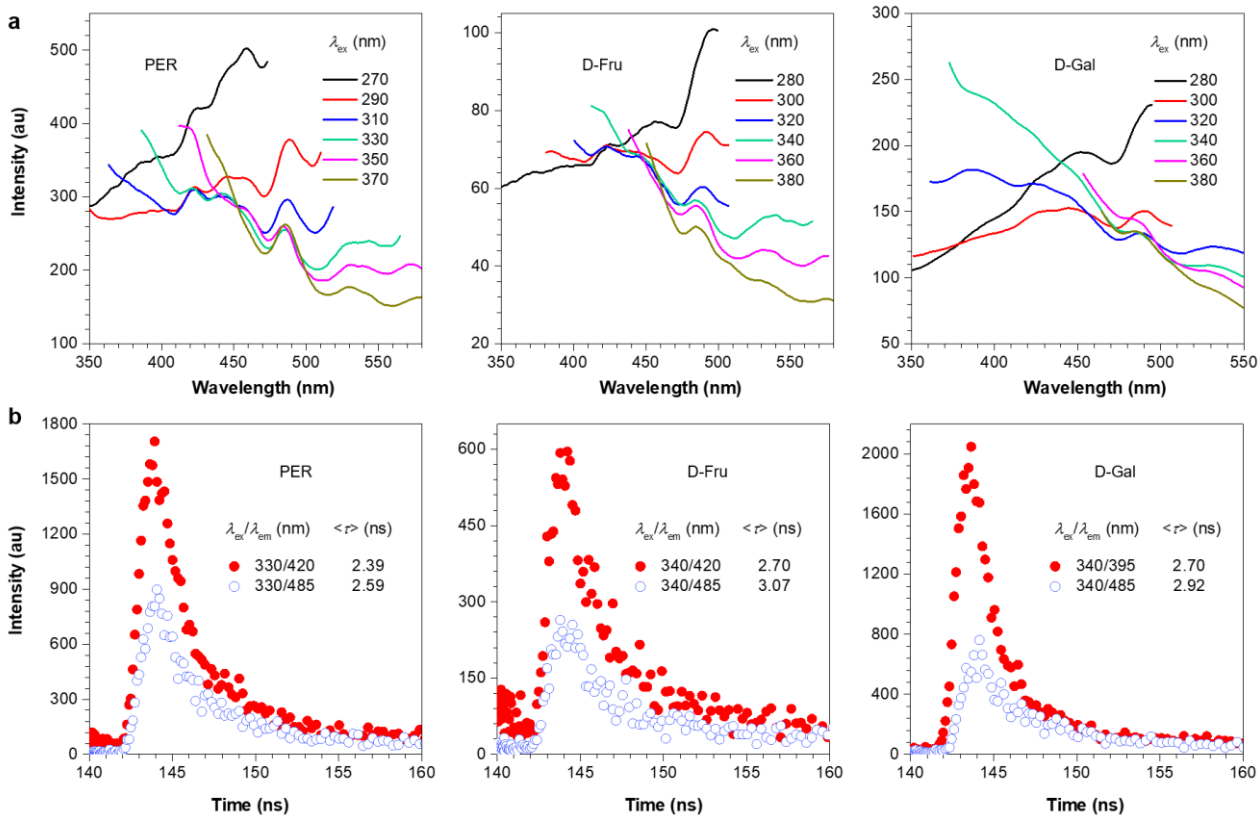

Fig. S13 (a) Emission spectra with different λ_{ex}s and (b) nanosecond scale lifetimes monitored at different wavelengths of the crystals of PER, D-Fru, D-Gal at room temperature.

Table S4 Summary of the *p*-RTP lifetimes of PER crystal excitation.[a]

τ_1 [ms]	A_1 [%]	τ_2 [ms]	A_2 [%]	τ_3 [ms]	A_3 [%]	τ [ms]	$\lambda_{ex,RTP}$ [nm]	$\lambda_{em,RTP}$ [nm]
30.8	18.6	239.0	44.3	1322.7	37.1	1119.2	255	500
20.4	24.3	208.0	39.4	1446.3	36.3	1268.9	285	515
20.5	26.4	180.7	42.4	1019.3	31.2	845.2	315	525

[a] All measurements were conducted at ambient conditions. $\lambda_{ex,RTP}$ = excitation wavelength used for the lifetime measurement; $\lambda_{em,RTP}$ = monitored emission wavelength. $\tau = (A_1\tau_1^2 + A_2\tau_2^2 + A_3\tau_3^3)/(A_1\tau_1 + A_2\tau_2 + A_3\tau_3)$.

Table S5 Summary of the *p*-RTP lifetimes of D-Fru crystal excitation.[a]

τ_1 [ms]	A_1 [%]	τ_2 [ms]	A_2 [%]	τ_3 [ms]	A_3 [%]	τ [ms]	$\lambda_{ex,RTP}$ [nm]	$\lambda_{em,RTP}$ [nm]
3.1	7.6	38.4	47.8	281.1	44.6	249.7	255	410
5.8	11.4	36.6	59.6	132.0	29.0	96.4	285	515
3.5	6.0	30.3	47.0	105.0	47.0	88.0	315	525

[a] All measurements were conducted at ambient conditions. $\lambda_{ex,RTP}$ = excitation wavelength used for the lifetime measurement; $\lambda_{em,RTP}$ = monitored emission wavelength. $\tau = (A_1\tau_1^2 + A_2\tau_2^2 + A_3\tau_3^3)/(A_1\tau_1 + A_2\tau_2 + A_3\tau_3)$.

Table S6 Summary of the *p*-RTP lifetimes of D-Gal crystal excitation.[a]

τ_1 [ms]	A_1 [%]	τ_2 [ms]	A_2 [%]	τ_3 [ms]	A_3 [%]	τ [ms]	$\lambda_{ex,RTP}$ [nm]	$\lambda_{em,RTP}$ [nm]
28.6	25.2	182.4	37.4	761.0	37	635.7	255	425
43.2	53.0	163.7	33.2	683.1	13.8	433.1	255	495
49.4	51.0	174.8	40.1	683.7	8.9	352.9	285	505
51.3	37.5	189.4	49.3	596.7	13.2	343.1	315	515

[a] All measurements were conducted at ambient conditions. $\lambda_{ex,RTP}$ = excitation wavelength used for the lifetime measurement; $\lambda_{em,RTP}$ = monitored emission wavelength. $\tau = (A_1\tau_1^2 + A_2\tau_2^2 + A_3\tau_3^3)/(A_1\tau_1 + A_2\tau_2 + A_3\tau_3)$.

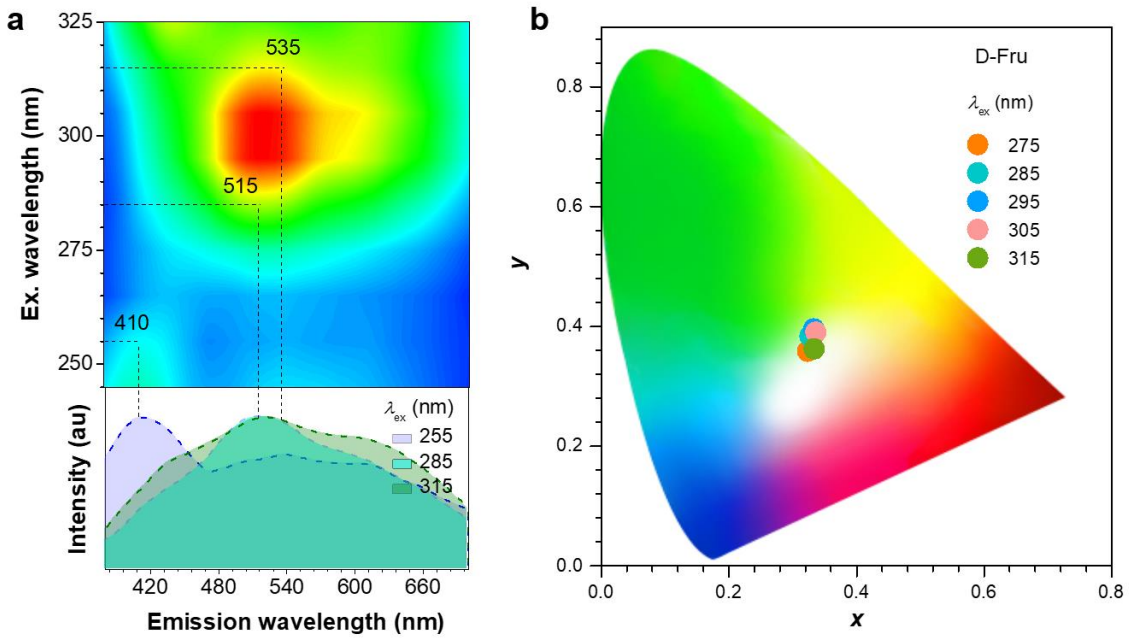

Fig. S14 (a) Excitation–p-RTP mapping of D-Fru crystals. The below inset shows the p-RTP spectra of D-Fru crystals, recorded under different λ_{ex} values (t_d = 0.1 ms). (b) Trajectory of tunable p-RTP emission colors, recorded on changing the λ_{ex} from 275 to 315 nm in the CIE coordinate diagram.

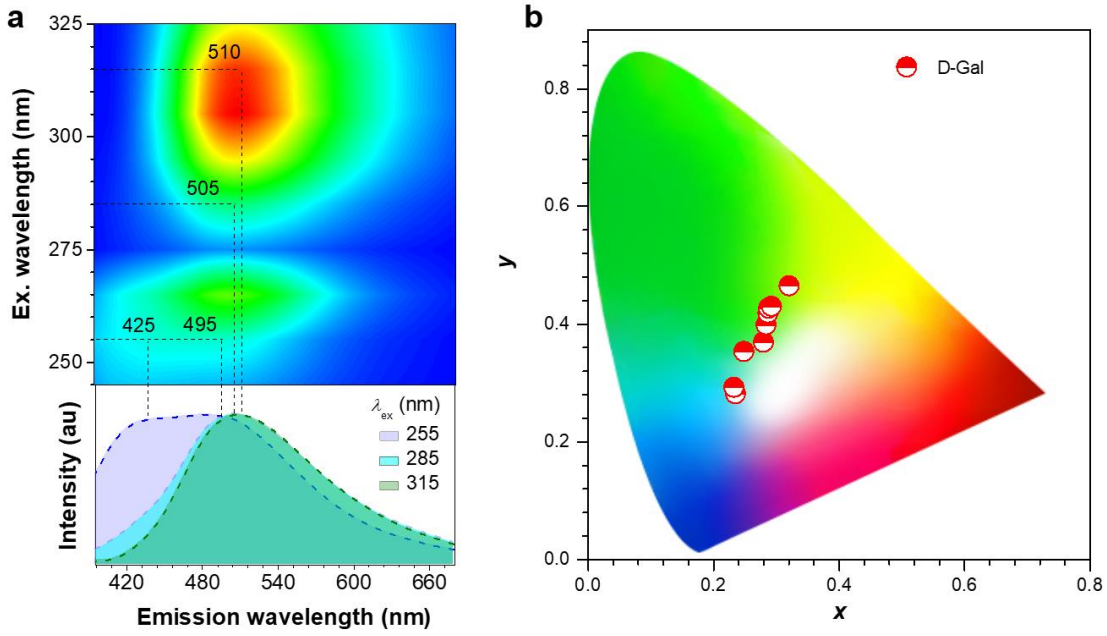

Fig. S15 (a) Excitation–p-RTP mapping of D-Fru crystals. The below inset shows the p-RTP spectra of D-Fru crystals, recorded under different λ_{ex} values (t_d = 0.1 ms). (b) Trajectory of tunable p-RTP emission colors, recorded on changing the λ_{ex} from 245 to 325 nm in the CIE coordinate diagram.

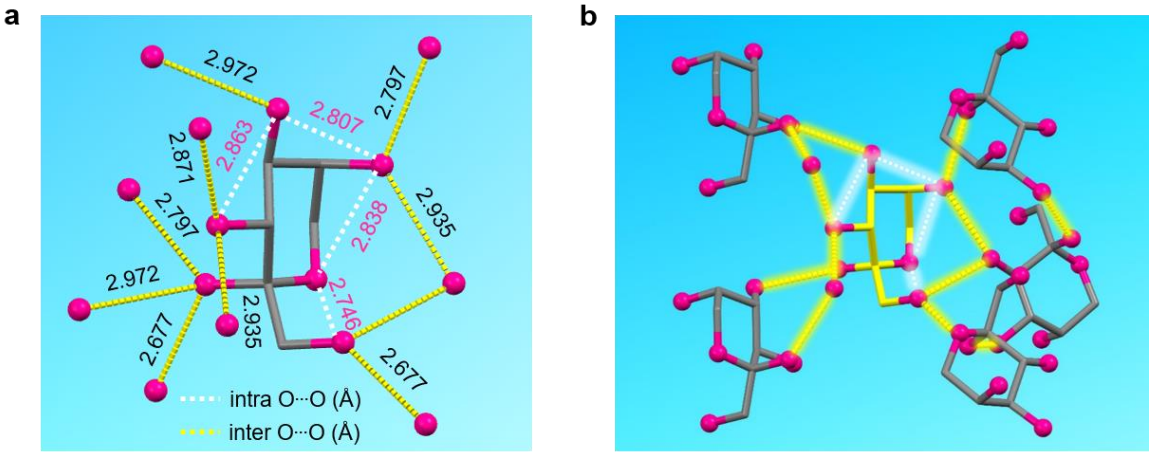

Fig. S16 (a) Single crystal structure of D-Fru with denoted intra- and intermolecular O···O interactions. (b) Fragmental molecular packing of PER in crystals with denoted O···O short contacts around one molecule.

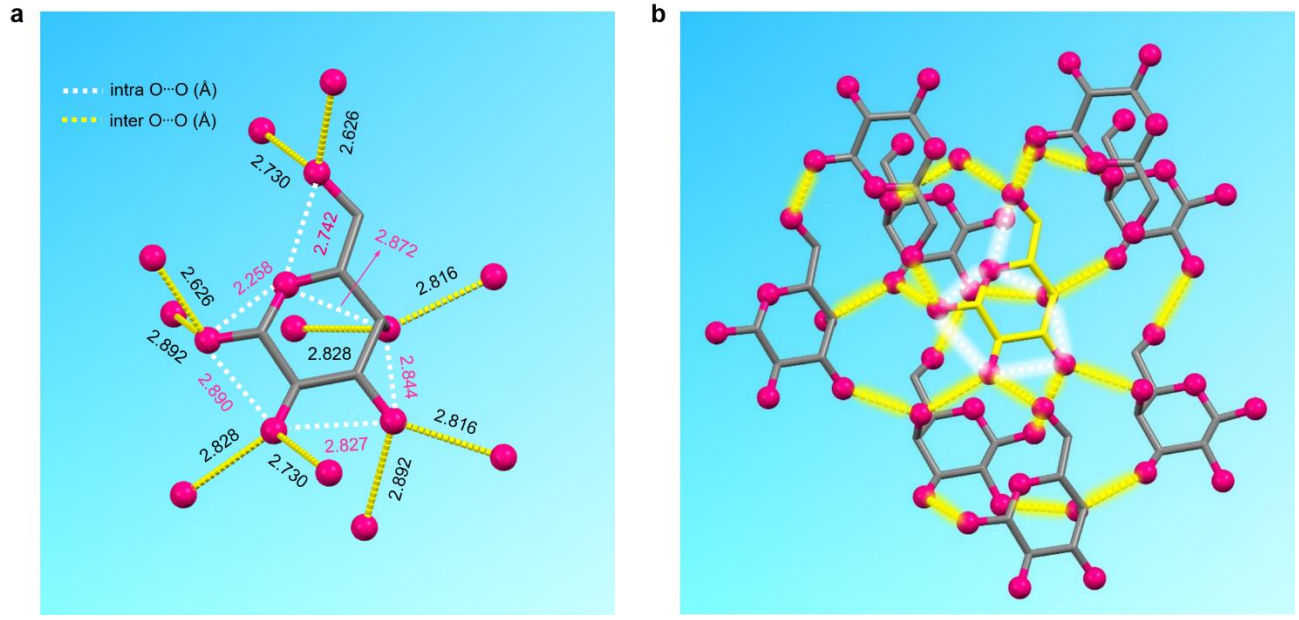

Fig. S17 (a) Single crystal structure of D-Gal with denoted intra- and intermolecular O···O interactions. (b) Fragmental molecular packing of D-Gal in crystals with denoted O···O short contacts around one molecule.

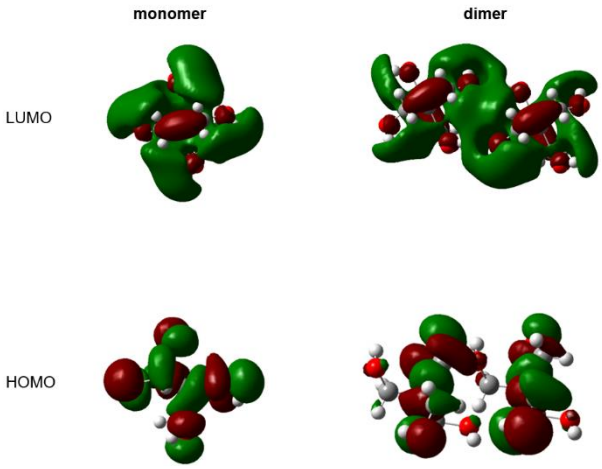

Fig. S18 HOMO and LUMO electron densities of the monomer and dimer for PER.

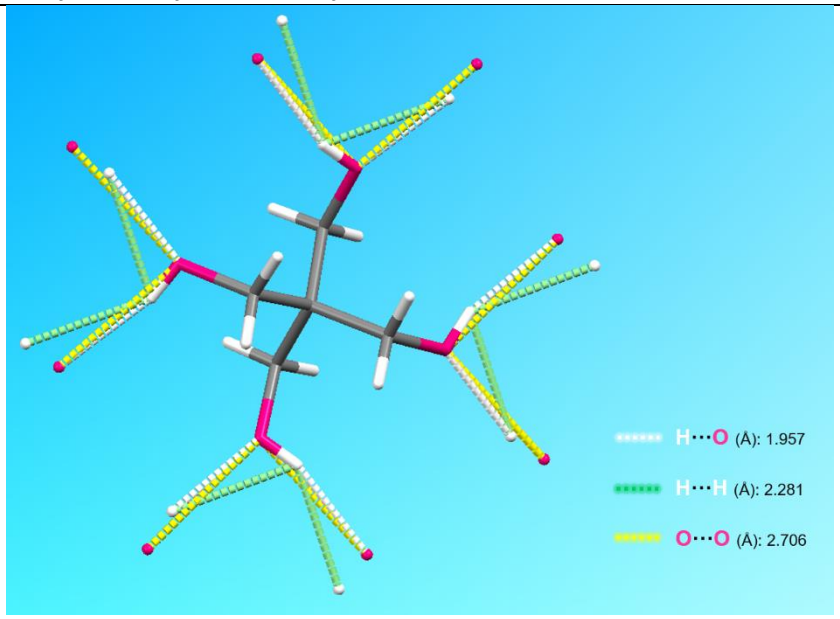

Fig. S19 Single crystal structure of PER with denoted intermolecular interactions.

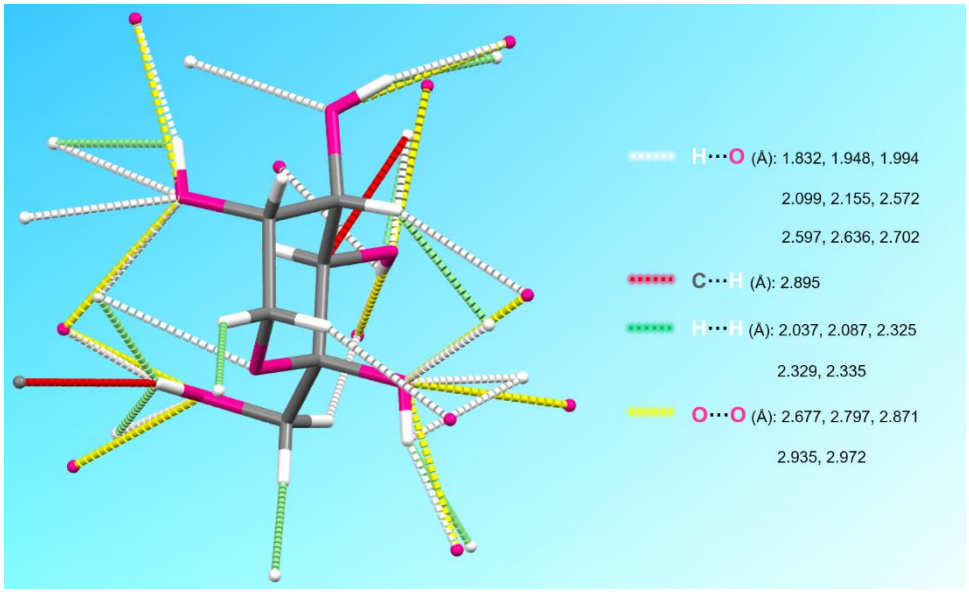

Fig. S20 Single crystal structure of D-Fru with denoted intermolecular interactions.

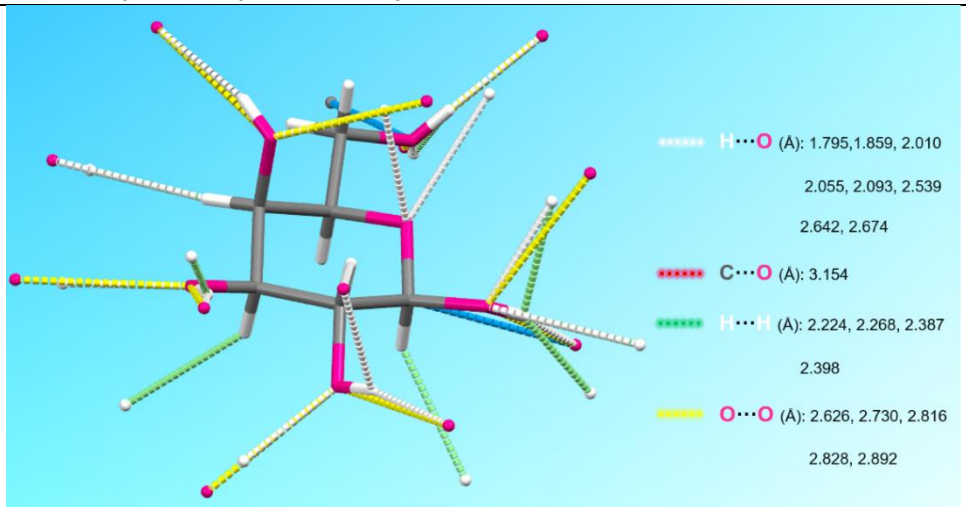

Fig. S21 Single crystal structure of D-Gal with denoted intermolecular interactions.

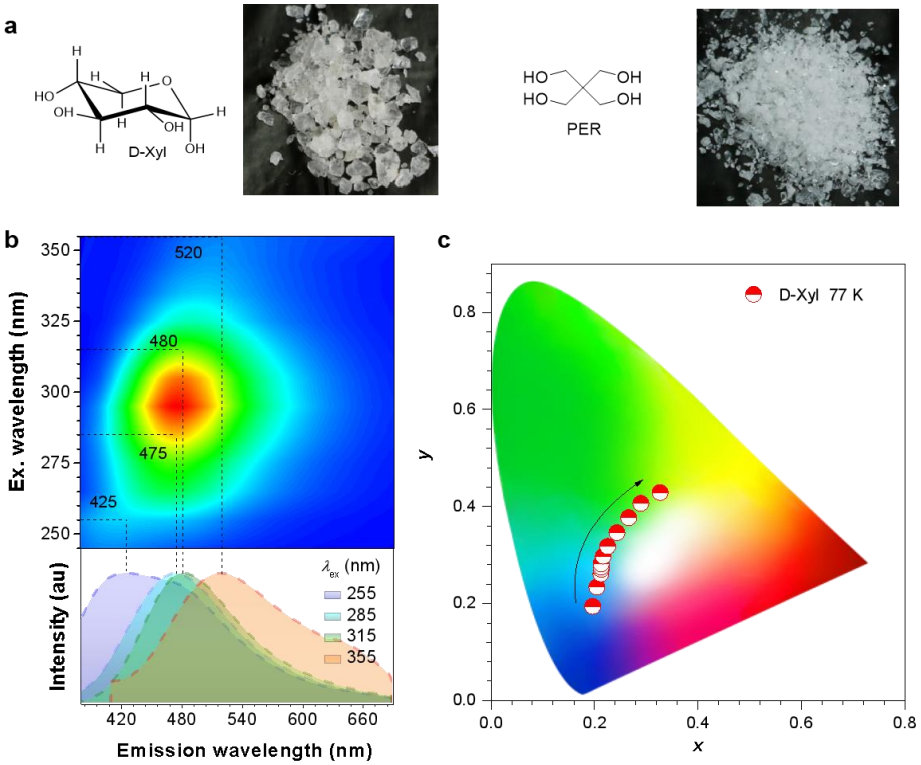

Fig. S22 (a) Photographs of D-Xyl and PER crystals taken under natural light at room temperature. (b) Excitation–phosphorescence mapping and the phosphorescence spectra with different excitations (t_d = 0.1 ms) of D-Xyl crystals at 77 K. (c) Trajectory of phosphorescence colors of D-Xyl crystals at 77 K, recorded by the change in the λ_{ex} from 245 to 355 nm, in the CIE coordinate diagram.